PRELIMINARY CLASSIFICATION RESULTS OF SIMULATED RADARSAT-2 POLARIMETRIC SEA ICE DATA

Bernd Scheuchl[(1)], Dean Flett[(2)], Gordon Staples[(3)], Gordon Davidson[(4)], Ian Cumming[(1)]

[(1)] Department of Electrical and Computer Engineering, University of British Columbia 2356 Main Mall, Vancouver, B.C. Canada V6T 1Z4 Email: bernds@ece.ubc.ca, ianc@ece.ubc.ca

[(2)] Canadian Ice Service/Ice & Marine Services Branch, Applied Science Division, 373 Sussex Drive, Block E, 3rd Floor, Ottawa, Ontario, Canada K1A OH3, Email: dean.flett@ec.gc.ca

[(3)] Radarsat International, 13800 Commerce Parkway, Richmond, B.C., Canada V6V 2J3, E-mail: gstaples@rsi.ca

[(4)] MacDonald Dettwiler and Associates, 13800 Commerce Parkway, Richmond, B.C., Canada V6V 2J3, E-mail: gordon@mda.ca

ABSTRACT / RESUME

When RADARSAT-2 is in operation it will be the first commercial spaceborne sensor capable of providing fully polarimetric data. The difference from airborne polarimetric data is mainly due to different sensor specifications and the differences in altitude. Using the airborne data, we simulate RADARSAT-2 standard and fine mode polarimetric data of sea ice and investigate the potential of ice classification algorithms. The increased noise level in combination with the lower resolution of the simulated data causes a decrease in classification quality compared to the airborne result and a change of classification strategy is required. However, the satellite polarimetric data does contain more information than the corresponding single polarization data, and can be exploited by new data processing techniques.

1 INTRODUCTION

RADARSAT-1 is an important information source for ice centres around the world, in their effort to provide accurate and timely sea ice information. In addition to the RADARSAT-1 capability, RADARSAT-2 will be the first commercial satellite capable of providing fully polarimetric data. In this paper, we investigate the potential of RADARSAT-2 polarimetric data for automated classification based on a simulation from airborne data.

Fig. 1 shows part of a RADARSAT-1 ScanSAR wide image acquired on March 8, 2001 over the Canadian East Coast. Climate reports for Moncton (New Brunswick) and Charlottetown (Prince Edward Island) from March 7, 8, and 9, 2001 indicate an average temperature in the area of approximately –4.2 degrees. In addition, the freezing degree-day parameter indicates an extended melt-free period prior to data acquisition. Analysis of the SAR data by the Canadian Ice Service shows an ice concentration >90%. The ice is generally classified as medium First Year Ice (70-120 cm thick) with floe sizes between 500 m and 2000 m. Using additional information like NOAA data, ice breaker and coastal observation, the ice chart shows a mix of ice types surrounding Prince Edward Island [40% grey ice (10-15 cm thick), 40% medium FYI (70-120 cm thick), 20% thin FYI (30-70 cm thick)]. Smaller floe sizes (between 20 m and 500 m) are reported.

Also on March 8, 2001, the Environment Canada CV-580 airborne SAR acquired fully polarimetric SAR data in the Northumberland Strait. The location of the flight line and the test site are shown in Fig. 1. An RGB colour composite using the channel information HH, HV and VV is shown in Fig. 2(i). The image covers 6.4 km in slant range and approximately 8 km in azimuth. The scene is available in SLC format and is used to simulate RADARSAT-2 polarimetric data.

The RGB composite image shown in Fig. 2(i) reveals the rich information content of the polarimetric data. Six classes can be identified due to different colouring of the image and this number is subsequently chosen for automatic image classification using an iterative Wishart classifier [1],[2]. More details on the classification are given in Section 3.

One important requirement for sea ice monitoring is area coverage. Fig. 1 illustrates the large difference in area coverage between the airborne acquisition and the RADARSAT-1 ScanSAR mode. While RADARSAT-2 polarimetric modes will only provide limited coverage (25 km swath) compared to the ScanSAR mode, the increased information content could be beneficial for the monitoring of ship traffic “hot spots” or for tactical ice breaker support.

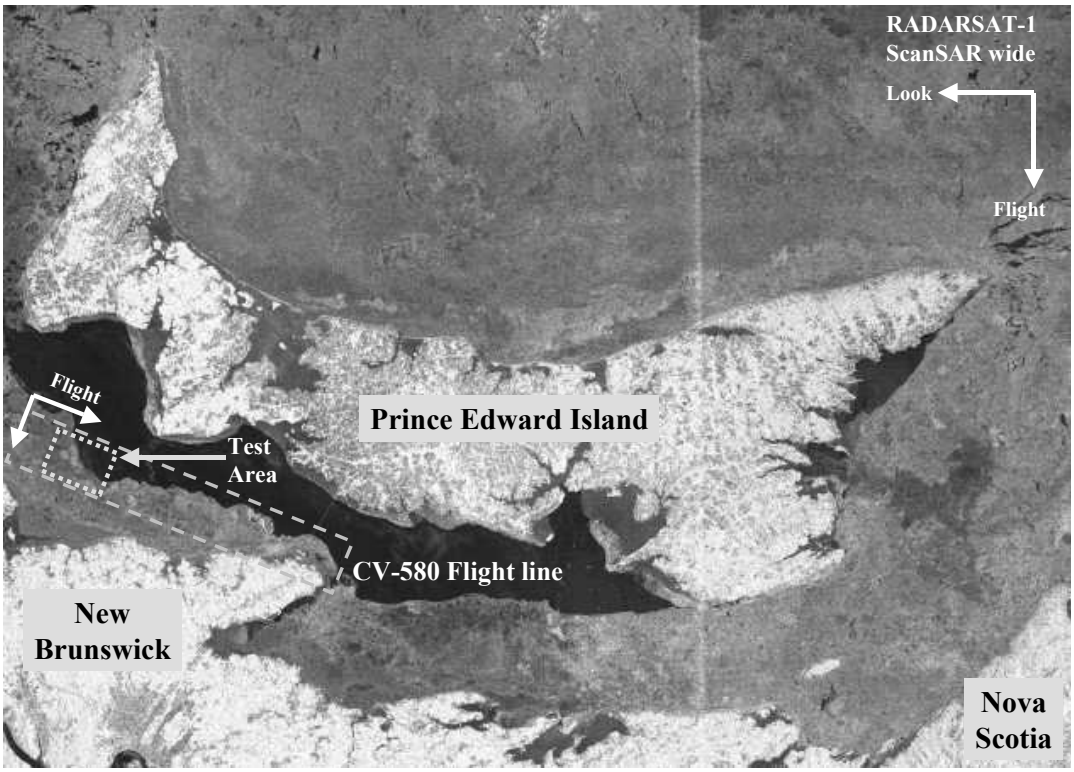

Fig. 1. RADARSAT-1 ScanSAR image (a 150 x 210 km subset of the full scene) acquired on March 8, 2001 over the Canadian East Coast. The bright areas in the image are land masses, the black areas are open water. The rest of the image shows sea ice coverage. The vertical streak is the nadir return that is unavoidable in some ScanSAR configurations. Also shown in this image are the flight line and test area (6.4 x 8 km) in the Northumberland Strait for CV-580 polarimetric data acquired by Environment Canada.

2 RADARSAT-2 DATA SIMULATION

The transformation from CV-580 SLC data to RADARSAT-2 SLC data has three components:

- Add zero mean complex Gaussian noise at the RADARSAT-2 NESZ level.
- Filter the complex airborne data in slant range and azimuth directions to reduce the bandwidth to equal the bandwidth of RADARSAT-2 data. This filtering represents a loss of information, applied to achieve the desired resolution and spectral shape of the simulated data. The filter inverts the assumed spectral shape of the input data, and applies a Kaiser window to simulate the spectral shape due to RADARSAT-2 processing. The filter is normalized to preserve statistics of the intensity values.
- Interpolation in the slant range and azimuth directions to the desired sample spacing.

After these operations, the simulated image has the same noise level, slant range and azimuth resolution and sample spacing as the anticipated RADARSAT-2 SLC images. If the input image is calibrated and the filters are properly normalized, then the output image is also calibrated. Table 1 shows the relevant image parameters.

Table 1. Image parameters for CV-580 and RADARSAT-2 SLC (polarimetric modes)

	CV-580	RADARSAT-2	
Parameter		Standard mode	Fine mode
Azimuth sample spacing	0.434 m	5.1 m	
Azimuth resolution	0.6 m	8 m	
Noise equivalent σ^0	-40 dB	-30 dB	
Slant range sample spacing	4 m	11.8 m	4.7 m
Slant range resolution	5 m	12.9 m	5.0 m
Incidence angle range	41° - 64°	20° - 49°	20° - 49°

Two differences from a real RADARSAT-2 SLC image remain in this approach. Firstly, the simulated image will be smaller than a real RADARSAT-2 image because of the limited range swath width of the CV-580 image (6.4 km vs. 25 km for RADARSAT-2). Also the ground range sample spacing will differ as the RADARSAT-2 simulated data is subsampled to the same slant range sample spacing. The incidence angle variation of the CV-580 data is large because of the low altitude and causes a geometric distortion of the simulated image compared to what a real RADARSAT-2 image would show. The difference in incidence angle coverage (see Table 1) will also have an impact on the backscatter observed. The difference in incidence angle range to the RADARSAT-2 incidence angle range will therefore affect polarimetric analysis results.

For classification purposes, the SLC data are multi-looked. Fig. 2 shows HH images as well as RGB composite images for CV-580 data (i), RADARSAT-2 standard simulation (ii) and fine mode simulation (iii). A target pixel size of approximately 15 m in each dimension was chosen for each data set, resulting in different levels of multi-looking for each scene. This in combination with the higher noise level and lower resolution of RADARSAT-2 data results in an increase in noise (grainy structure) from Fig. 2(i) to Fig. 2(iii). Due to the significantly higher resolution of the airborne data, the ratio of looks between the airborne data and the RADARSAT-2 standard data is about 18, which affects the distribution of the measured parameters.

A comparison of the RGB composite image to their HH counterparts clearly shows that the polarimetric data carry more information about the target area than single polarization data. Visual interpretation shows six different ice types in the scene. The six classes are discussed in more detail in Section 3. Despite an increase in noise, the RGB composites of the RADARSAT data appear to retain much of the spatial information.

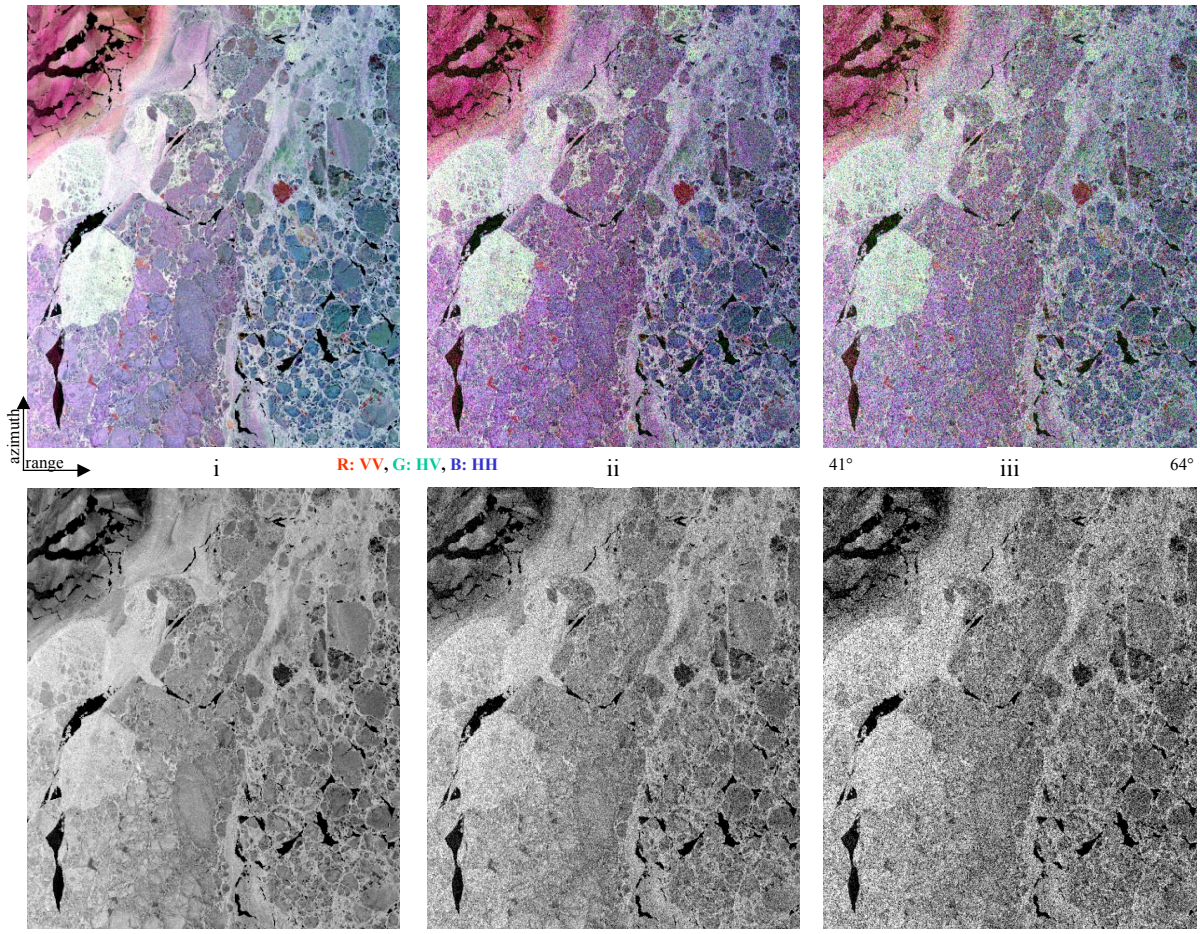

Fig. 2. RGB composite images using channel intensities (top row) and HH images (bottom row).
(i) CV-580; Multi-looking: azimuth 40, range 4; Pixel size: azimuth 17.35 m, range: 16 m
(ii) RADARSAT-2 fine; Multi-looking: azimuth 3, range 3; Pixel size: azimuth 15.3 m, range: 14.2 m
(iii) RADARSAT-2 standard; Multi-looking: azimuth 3, range 1; Pixel size: azimuth 15.3 m, range: 11.85 m.

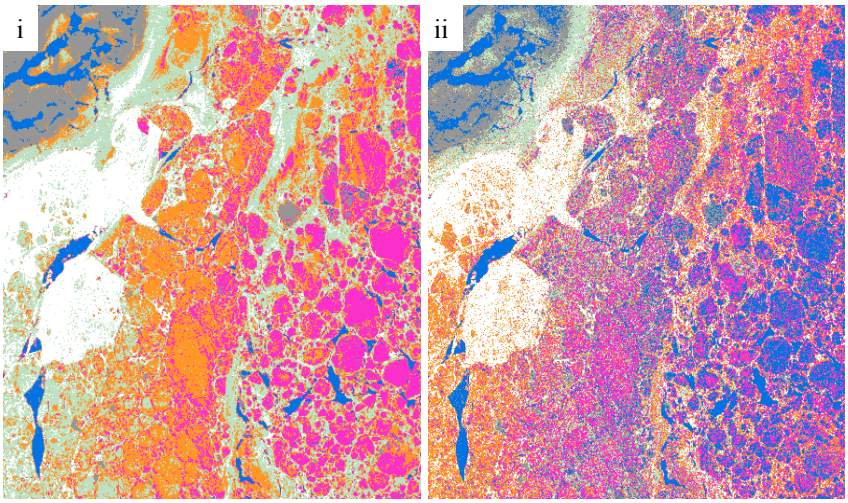

Fig. 3. Iterative Wishart classification result.
(i) CV-580; multilooking: azimuth 40, range 4 (see Tab. 2 for colour assignment);
(ii) RADARSAT-2 fine; multilooking: azimuth 3, range 3.

Tab. 2. Colour assignment for the CV-580 classification result (see Fig. 3(i))

Class #	**Colour**	**Ice Type**
1	Grey	Thin, new forming ice (ThI)
2	Magenta	FYI (floes, far range)
3	White	rough FYI (strong HV)
4	Green	ridged FYI
5	Blue	Leads
6	orange	FYI (floes, near range)

3 CLASSIFICATION OF SIMULATED DATA

The original data and the RADARSAT-2 fine simulation are classified using an iterative Wishart classifier with a six-class initialization. Six classes were chosen following a visual analysis of the CV-580 RGB composite image. The classification results are shown in Fig. 3 and an interpretation of the classes for the reference result (Fig. 3(i)) is given in Tab. 2. The colour assignment for the RADARSAT-2 result was chosen to closely resemble the reference solution. Due to the differences in the two results, class confusion is present compared to the airborne result. A more detailed description of the classification algorithm can be found in [3].

For the CV-580 data classification (Fig. 3(i)) a modified H/α classifier was chosen to initialize the Wishart classifier [3]. Fig. 3 (ii) shows a classification using an image with six classes randomly distributed to initialize the Wishart classifier. The modified H/α classifier was not chosen here because of the low level of multi-looking for the scene affecting H/α parameter estimation. Previous research shows that both initializations should lead to very similar results [4].

In comparison to the CV-580 classification result (Fig. 3(i)) class confusion, overestimation of leads and a very noisy result are easily visible for the RADARSAT-2 classification. Most critical is the apparent confusion between far range floes (smooth FYI) and leads. This makes this result unreliable for ice concentration measurement when using the same classification method as for airborne data.

4 EFFECT OF NOISE ON CLASSIFICATION CAPABILITY

In order to understand the differences in the classification results, it is useful to examine the distribution of some of the key features between the two data sets. 2-D scatter plots of the entire data sets are used for a comparison between the RADARSAT-2 fine simulation and the original data. The distribution of three parameters vs. HH are shown in Fig. 4. The CV-580 classification result (Fig. 3(i), Table 2) was used for both data sets to group the data into classes and

calculate the mean and standard deviation for each class (shown as crosses in Fig. 4). For the RADARSAT-2 simulated data, each sample was assigned the class of the nearest sample in the CV-580 image.

Using 2-D scatter plots, class separation for a single feature or a feature pair can be investigated. While the CV-580 scatter plots show reasonable class separation, the RADARSAT-2 scatter plots do not. Higher dispersion of the classes can be observed in the RADARSAT-2 case owing to higher noise levels and fewer looks. Detailed comments on the scatter plots are given in the next four paragraphs.

The co-polarized scatter plot shows that the increased noise level affects both HH and VV channels in the RADARSAT-2 case. The mean of class 5 (leads), which is well separated from the rest for the airborne data is now higher, more so for HH than for VV. The smaller increase in VV indicates that information that was picked up in the airborne case is now masked in the noise. This will certainly affect the ability for ice-water separation. Due to increased speckle, the pixels do not form separate "clouds" for the simulated data (right plot) as they do for the airborne data (left plot) and the error bars increase in size thus causing significant overlap between classes.

The co-pol ratio distribution in row two shows the same problem. Where a simple ratio threshold was sufficient to separate classes 1 and 5 (THI and leads) from FYI for the airborne data, this threshold is not longer obvious in the simulation case (i.e. no separation of clouds and overlap of error bars). Error bar overlap happens not only between neighbouring classes but affects now up to 4 classes. Class 5 is most affected by the increased noise level and shows a higher average ratio than class 1.

The magnitude of the complex correlation coefficient in row three also shows an increase in the standard deviation, although, the mean values appear relatively unchanged. Again no separated clouds can be seen in the simulated data.

Leads (class 5) appear to be severely affected by the increased noise level, which shows in practically all parameters presented here. Backscatter from leads is largely masked by the increased noise of the RADARSAT-2 data. Because the increase in the average VV is smaller than for HH, the airborne data indeed picked up a signal from leads. This information is not available for the simulated RADARSAT-2 data. Changes in classification strategy are therefore needed for RADARSAT-2 data.

5 CONCLUSIONS

Simulation of RADARSAT-2 data from airborne data requires a change in resolution and noise level. Differences that cannot be taken into account are a different incidence angle range and lower data coverage of the airborne data.

In this paper, we compare the simulated data to a high-resolution airborne product and find that the same classification performance cannot be expected. However, RADARSAT-2 polarimetric data still carries more information than a comparable single polarization product, and we must continue to seek better ways of exploiting it.

The Wishart classifier as set up for airborne data does not perform as well for the simulated data with extra noise and fewer looks. Existing strategies for classification of airborne polarimetric SAR data will need to be optimized to account for differences in noise level and resolution. More data sets will be studied, including those with more ice types. Final adjustments will be needed once real RADARSAT-2 data become available.

Finally, note that the limited coverage of polarimetric modes is not ideal for ice monitoring purposes. It is expected that ScanSAR modes (possibly with dual polarization) will continue to be the main resource for ice monitoring, although polarimetric modes will be useful where detailed information over a smaller area (e.g. ship traffic hotspots) is desired.

6 ACKNOWLEDGEMENTS

The authors thank the Canadian Space Agency and Environment Canada for providing data. This work was funded by MacDonald Dettwiler and Associates under contract to the Canadian Space Agency (No. 9F028-0-4902/06) as part of the Earth Observation Applications Development Program.

7 REFERENCES

1. Pottier E. and Lee J.S., Application of the H/A/α Polarimetric Decomposition Theorem for Unsupervised Classification of Fully Polarimetric SAR Data Based on the Wishart Distribution, *CEOS'99*, Toulouse, France, 1999.

2. Ferro-Famil L., Pottier E., and Lee J.S., Unsupervised Classification of Multifrequency and Fully Polarimetric SAR Images Based on the H/A/Alpha–Wishart Classifier, *IEEE Transactions on Geoscience and Remote Sensing*, vol. 39, no. 11, pp. 2332-2342, November 2001.

3. Scheuchl B., Hajnsek I., Cumming I.G., Classification strategies for fully polarimetric SAR data of sea ice, *POLinSAR* (these proceedings), Frascati, Italy, Jan 14-16, 2003.

4. Scheuchl B., Hajnsek I., Cumming I.G., Sea Ice Classification Using Multi-Frequency Polarimetric SAR Data, in *Proc. IGARSS'02*, Toronto, June 2002.

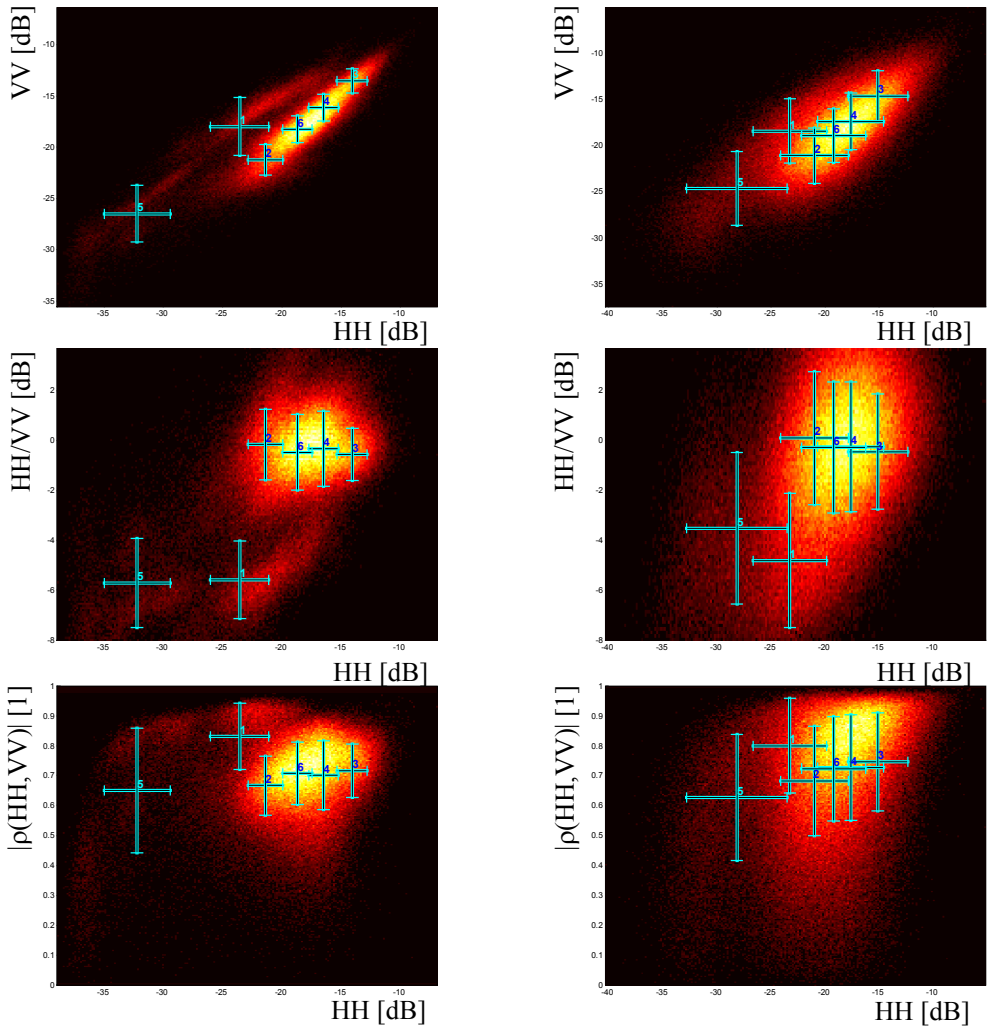

Fig. 4. 2-D scatterplots with colour coded density information.
Left side: CV-580 data, 40x4 looks; Right side: simulated RADARSAT-2 fine mode data, 3x3 looks
The crosses indicate the class means and standard deviations based on the reference solution derived from the CV-580 data using an iterative Bayesian classifier (see Fig. 3(i), and Tab. 2).